

NEURAL COMPUTING OF THE BANDWIDTH OF RESONANT RECTANGULAR MICROSTRIP ANTENNAS

Şeref Sağıroğlu⁺, Kerim Güney^{*} and Mehmet Erler^{*}

(⁺) Intelligent Systems Research Group, Erciyes University, Engineering Faculty, Control & Computer Engineering Department, 38039, Kayseri, Turkey, SS@ZIRVE.ERCIYES.EDU.TR.

(^{*}) Intelligent Antenna Design Research Group, Erciyes University, Engineering Faculty, Electronic Engineering Faculty, 38039, Kayseri, Turkey.

Abstract: A new method based on the backpropagation multilayered perceptron network for calculating the bandwidth of resonant rectangular microstrip patch antennas is presented. The method can be used for a wide range of substrate thicknesses and permittivities, and is useful for the computer-aided design (CAD) of microstrip antennas. The results obtained by using this new method are in conformity with those reported elsewhere. This method may find wide applications in high-frequency printed antennas, especially at the millimeter-wave frequency range.

1. INTRODUCTION

Microstrip antennas have sparked interest among researchers because of their many advantages over conventional antennas, advantages such as low cost, light weight, conformal structure, low profile, reproducibility, reliability, ease in fabrication and integration with solid-state devices, etc. [1-12].

Consider a rectangular patch of width W and length L over a ground plane with a substrate of thickness h and a relative dielectric constant ϵ_r , as shown in Fig.1. In rectangular microstrip antenna designs, it is important to determine the bandwidth of the antenna accurately because the bandwidth is a critical parameter of a microstrip antenna.

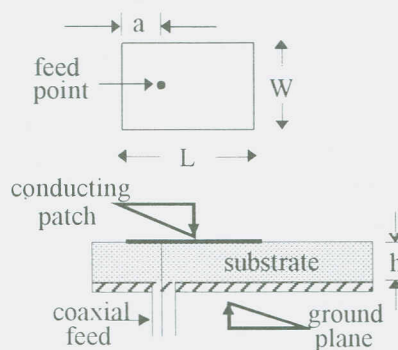


Figure 1. Geometry of a rectangular microstrip antenna

A number of attempts [1-8] have been made to determine the bandwidth of rectangular microstrip antennas, as this is one of the popular and convenient shapes. However, most of the previous theoretical and experimental work has been carried out only with electrically-thin rectangular microstrip antennas, normally of the order of $h/\lambda_d \leq 0.02$, where λ_d is the wavelength in the substrate. Recently interest has developed in radiators etched on

is the fact that microstrip antennas are currently being considered for use in millimeter-wave systems. The substrates proposed for such applications often have high relative dielectric constants and, hence, appear electrically thick. The need for greater bandwidth is another major reason for studying thick substrate microstrip antennas. Consequently, this problem, particularly the bandwidth aspect, has received considerable attention.

Some popular methods, such as the cavity model methods [1] (radiation losses are included in the effective loss tangent of the dielectric) and the transmission line models [1] (radiation losses are included in the attenuation coefficient of the propagation constant) are simple and successful in the analysis of microstrip antennas, and therefore in calculating the bandwidth of rectangular microstrip patch antennas. However, these models are valid for electrically thin microstrip antennas.

A practical algorithm for calculating the bandwidth has been developed by Carver [2] for implementation on a computer. However, this involves computations via a nonlinear difference scheme, and it is not presented by a simple unique expression.

The most important of the results published is by Pozar [4]. He presented bandwidth against normalized substrate thickness. The bandwidth data calculated by using the moment method approach were presented by [4] for rectangular microstrip antennas on substrates which may be electrically thick, as would be the case for microstrip antennas at millimeter wave frequencies.

One of certain ways of calculating the bandwidth of a rectangular microstrip antenna involves the evaluation of a double integral. Among others, this approach has been introduced by [6]. A certain current distribution is assumed along the upper conductor which is typical of the geometry of the element. The current in the radiating element is obtained by using cavity or equivalent transmission line models. The electric field is derived from the assumed current distribution using the appropriate Green's function. The radiated power is found by integration of field. The bandwidth of a rectangular microstrip antenna is then obtained by using the formula given in [6]. Perlmutter et al. [6] also considered cases other than those considered by Pozar [4]. The results obtained by [5] confirmed the results obtained by [4], but they did not provide extra material. However, the methods in [4-6] are very complicated and rigorous.

Güney [8] proposed a closed-form expression for the bandwidth of rectangular microstrip antennas. This expression was derived from numerical results available in the literature and provides insight into the fundamental influence of the substrate parameters on the bandwidth.

From the studies cited above we see that the certain way of calculating the bandwidth of rectangular microstrip antennas involves the complicated Green's function methods and integral transformation techniques [1,4-6].

Artificial neural networks (ANNs) are known to provide simpler and faster solutions than the complicated methods and techniques. The features of ANNs such as ability and adaptability to learn, generalisation, less information requirement, fast real-time operation and ease of implementation have made them popular in recent years [13,14]. Because of these fascinating features, ANN models have been applied in many areas. In previous works [15-18], we successfully introduced a neural model to compute the resonant frequency of the triangular and circular microstrip antennas and the resonant resistance of rectangular microstrip antennas.

This article presents a new model based on the backpropagation multilayered perceptron network to find accurately the bandwidth of both electrically thin and thick rectangular microstrip antennas. This proposed neural model does not require the complicated Green's function methods and integral transformation techniques. The model

only requires three parameters: W/λ_0 , h and ϵ_r . The results obtained from this model are in excellent agreement with the results available in the literature even when $h(\epsilon_r)^{1/2}/\lambda_0 = 0.15$.

2. BANDWIDTH OF RECTANGULAR MICROSTRIP ANTENNAS

The input impedance of this antenna, which can be modeled by a simple parallel-resonant RLC circuit, can be expressed as [1,7]

$$Z_{in} = \frac{R}{1 + jQ_T v} \quad (1)$$

with

$$v = \frac{f}{f_r} - \frac{f_r}{f} \quad (2)$$

where R is the resonant resistance, Q_T is the total quality factor, f is the frequency variable, and f_r is the resonant frequency. In the vicinity of its fundamental resonant frequency, the input impedance of a microstrip antenna can also be modeled by a series-resonant RLC circuit. In the series-resonant case, the input impedance is given by

$$Z_{in} = R(1 + jQ_T v) \quad (3)$$

The input VSWR can be written as

$$\left| \frac{Z_{in}(f) - Z_0}{Z_{in}(f) + Z_0} \right| = \frac{VSWR(f) - 1}{VSWR(f) + 1} \quad (4)$$

where Z_0 is the characteristic impedance of the feed line. If the bandwidth criterion is taken to be $VSWR \leq s$, and f_1 and f_2 are the lower and upper band edge frequencies, respectively, so that $VSWR(f_1) = VSWR(f_2) = s$, the bandwidth is given as

$$BW = \frac{f_2 - f_1}{f_r} \quad (5)$$

From (1)-(5), the following equation is obtained

$$BW = \frac{1}{Q_T} \left[\frac{(Ts - 1)(s - T)}{s} \right]^{1/2} \quad (6)$$

where $T = Z_0/R$ in the series-resonant case, and $T = R/Z_0$ in the parallel-resonant case. Because, normally, an antenna is designed to be perfectly matched at its resonant frequency (e.g., by properly locating the position of a coaxial feed probe or by using a quarter-wavelength transformer), T normally equals unity. (6) then becomes the following expression

$$BW = \frac{s - 1}{Q_T \sqrt{s}} \quad (7)$$

The total quality factor, Q_T , can be written as

$$\frac{1}{Q_T} = \left[\frac{1}{Q_r} + \frac{1}{Q_c} + \frac{1}{Q_d} + \frac{1}{Q_s} \right] \quad (8)$$

where the four terms represent the radiation quality factor, the quality factors due to conductor loss, dielectric loss and surface wave. Although, Q_d and Q_c are easily found, Q_r and Q_s has to be obtained using the complicated Green function methods and integral transformation techniques [1,4-6]. These methods and techniques suffer from a lack of computational efficiency, which in practice can restrict their usefulness because of high computational time and costs.

Bandwidth was defined by Pozar [4] as the half-power width of the equivalent circuit impedance response. For a series-type resonance, this bandwidth is

$$BW = \frac{2R}{w_r \left. \frac{dX}{dw} \right|_{w_r}} \quad (9)$$

where $Z=R+jX$ is the input impedance at the radian resonant frequency w_r . For a parallel-type resonance, (9) is used with R replaced by G and X replaced by B , where $Y=G+jB$ is the input admittance at resonance. This definition of bandwidth implies a standing wave ratio of about 2.4, for a transmission line of characteristic impedance R or $1/G \Omega$. The derivative in (9) can be evaluated by calculating the input impedance at two frequencies near resonance and using a finite difference approximation. The resonant resistance, R , is given by

$$R = R_r + R_d + R_c + R_s \quad (10)$$

where the four terms represent the radiation resistance, the equivalent resistance of the dielectric loss, the equivalent resistance of the conductor loss, and surface wave radiation resistance. Although, R_d and R_c are easily found, R_r and R_s has to be obtained using the rigorous numerical methods [1,4-6]. These methods require high performance large-scale computer resources and a very large number of computations.

In this paper, we will concentrate on the bandwidth results reported by Pozar [4] and Perlmutter et al. [6]. Because the results presented by Pozar [4] and Perlmutter et al. [6] agree with those presented by other scientists in the literature. The results calculated by [6] using the electric surface current model are presented in Figs. 4-7 for $\epsilon_r=1.1, 2.2$ and 9.8 . The results calculated by Pozar [4] using a moment method approach for a substrate with relative permittivity $\epsilon_r=2.55$ and $W/\lambda_0=0.3$ are given in Fig. 8. The graphs refer to end feed resonant rectangular elements that is to elements whose length is half a wavelength in the microstrip. The feeding method or position does not effect the intrinsic patch bandwidth. It was shown by Pozar [4] that the bandwidth of a patch is significantly greater than that of a printed dipole, at least over the range for which the patch actually resonates ($h < 0.11\lambda_0$). Therefore, the effect of the patch width W on the bandwidth of rectangular microstrip antennas must be taken into consideration in the bandwidth calculation of these antennas. From the plots we see that for a given frequency, larger bandwidth is possible by choosing a thicker substrate and a wider patch. The curves also indicate that a lower value of ϵ_r results in a larger bandwidth. As we are only interested in resonant antennas, the physical length L of the patch is not of importance: it is determined by

$$L = \frac{c}{2f_r \sqrt{\epsilon_e}} - 2\Delta L \quad (11)$$

where c is the velocity of electromagnetic waves in free space, ϵ_e is the effective relative dielectric constant for the patch, f_r is the resonant frequency, and ΔL is the edge extension. ϵ_e and ΔL depend on ϵ_r , h , and W . Thus the length L is determined by W , h , ϵ_r , and f_r . Therefore only three parameters, h , W/λ_0 and ϵ_r , are needed to describe the bandwidth. These parameters are used for neural calculation of the bandwidth.

In the following section, the backpropagation multilayered perceptron network used in this paper is briefly described and the neural model for calculating the bandwidth of a microstrip antenna is then explained.

3. BACKPROPAGATION MULTILAYERED PERCEPTRON NETWORKS

Multilayered perceptrons (MLPs) which are among the simplest and therefore most commonly used network structures have been adapted for many applications [13,19]. Fig. 2 shows an MLP with three layers: an input layer, an output layer and an intermediate or hidden layer. The circles and the connection lines in the figure represent neurons and weights, respectively. The biases are not shown in the figure. Each layer consists of a number of

neurons. All the neurons in a layer are fully connected to the neurons in adjacent layers but there is no connection between the neurons within the same layer. Each connection has an unbounded positive and negative weight associated with it. The output of multilayered perceptron is a function of the inputs and the weights.

Inputs to the network are passed to each neuron in the input layer. The outputs of the neurons in the first layer become inputs to the hidden layer and so on. Neurons in the input layer only act as buffers for distributing the input signals x_i to neurons in the hidden layer. Each neuron j in the hidden layer sums up its input signals x_i after weighting them with the strengths of the respective weight connections w_{ji} from the input layer and computes its output y_j , which is the output of the j -th neuron in the hidden or output layer, as a function f of the sum,

$$y_j = f(\text{net}_j) \quad (12)$$

with

$$\text{net}_j = \sum_i w_{ji} x_i + \theta_j \quad (13)$$

where f is a transfer or activation function and can be a sigmoid or a hyperbolic tangent function, and θ_j is a variable bias with similar function to a threshold. The transfer function has the feature of being nondecreasing and differentiable, and the range of y_j is between -1.0 and 1.0 for the tangent hyperbolic function.

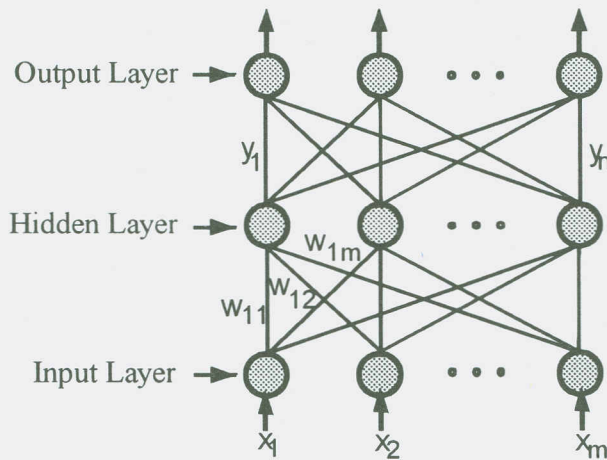


Figure 2. Topology of multilayered perceptron

Note that y_j can be defined recursively in terms of its inputs. The computation continues until the output of the network is found. After computing the output, the training process starts in according with the learning algorithm used.

MLPs can be trained using many different learning algorithms. For simplicity, the standard backpropagation learning algorithm [19] has been selected for training in this work. It is a gradient descent algorithm. Basically, the learning in an MLP is to find a set of weights that minimizes the mismatching between the network outputs and the target values. It is an iterative training process in which an output error is propagated back through the layers and used to modify weights. The error E is defined by

$$E = \sum_p E_p = \frac{1}{2} \sum_p \sum_i (ty_{pj} - y_{pj})^2 \quad (14)$$

where ty_j is the desired or target value of output for a given input, and the summation is performed over all output neurons j . Once the outputs from the hidden layers and output

layer have been calculated for each input pattern p , the direction of steepest descent in parameter space is determined by the following partial derivatives of E

$$-\frac{\partial E}{\partial w_{ji}} = \sum_p \delta_{pj} y_{pi} \quad (15)$$

$$-\frac{\partial E}{\partial \theta_j} = \sum_p \delta_{pj} \quad (16)$$

where δ_{pj} can be calculated as

$$\delta_{pj} = -\frac{\partial E_p}{\partial net_{pj}} = -\frac{\partial E_p}{\partial y_{pj}} \frac{\partial y_{pj}}{\partial net_{pj}} \quad (17)$$

with

$$\frac{\partial y_{pj}}{\partial net_{pj}} = (1 - y_{pj})(1 + y_{pj}) \quad (18)$$

$$\frac{\partial E_p}{\partial y_{pj}} = \frac{\partial}{\partial y_{pj}} \sum_j \frac{1}{2} (ty_{pj} - y_{pj})^2 = -(ty_{pj} - y_{pj}) \quad (19)$$

$$\frac{\partial E_p}{\partial y_{pj}} = \sum_k \frac{\partial E_p}{\partial net_{pk}} \frac{\partial net_{pk}}{\partial y_{pj}} = -\sum_k \delta_{pk} w_{kj} \quad (20)$$

(19) and (20) are, respectively, valid for the output and hidden neurons. (20) also shows how the analysis proceeds from the output layer to the preceding layers. So the quantities δ_{pj} can be calculated in parallel for all output neurons j as

$$\delta_{pj} = (ty_{pj} - y_{pj})(1 - y_{pj})(1 + y_{pj}) \quad (21)$$

The following quantities δ_{pj} for all hidden layer can be then written by using (17)

$$\delta_{pj} = (1 - y_{pj})(1 + y_{pj}) \sum_k \delta_{pk} w_{kj} \quad (22)$$

where j refers to a neuron in one of the hidden layers, and the summation is over all neurons k , which receive signals from neuron j .

Substituting (21) and (22) into (15) and (16), the steepest descent direction from a current weight bias configurations is obtained. The weights w_{ji} and biases θ_j are changed according to the following equations

$$\Delta w_{pj}(t) = \alpha \sum_p \delta_{pj} y_{pi} + \beta w_{kj}(t-1) \quad (23)$$

$$\Delta \theta_j(t) = \alpha \sum_p \delta_{pj} + \beta \theta_j(t-1) \quad (24)$$

where t indexes the number of times to train the neural model, α is the learning coefficient, β is the momentum coefficient which determines the effect of past weights' changes on the current direction of movement in the weight surface.

A good choice of β and α is essential for training process success and speed. The backpropagation learning is strongly affected by these two coefficients. Good values for the coefficients must be determined empirically. They depend on applications [20] or problems [21]. The typical good values for learning coefficient are between 0.01 and 0.9. For complicated tasks, the coefficient may be chosen as a small value [22].

Training an MLP by backpropagation to compute BW involves presenting it sequentially with different $(h, W/\lambda_o$ and $\varepsilon_r)$ tuples and corresponding target values. Errors between the target output and the neural model output are backpropagated through the network to adapt its weights using (14)-(24).

The training explained above is known as pattern-based training, as opposed to batch training where the weights are only modified once all the tuples in the training set have been presented to the network. Pattern-based training was adopted in this work as it is faster than batch training.

A training epoch is completed after all tuples (sets) in the training set applied to the network. Training stops when the bandwidth accuracy of the network is deemed satisfactory according to some criterion such as the root-mean-square (rms) error between the target bandwidth and neural model output for all the training set falls below a given threshold or the maximum allowable number of epochs is reached.

4. NEURAL COMPUTING OF THE BANDWIDTH, SIMULATION RESULTS AND DISCUSSIONS

The neural model for calculating BW is shown in Fig. 3. In the figure, LF and TF represent the linear activation function and the tangent hyperbolic function used in the MLP structure, respectively.

A set of random values distributed uniformly between -0.1 and +0.1 was used to initialise the weights of the networks. The tuples were scaled between -1.0 and +1.0 before training. The neural models used in this paper had two hidden layers as this number of hidden layers should be sufficient for a neural network to perform such calculations [22-25].

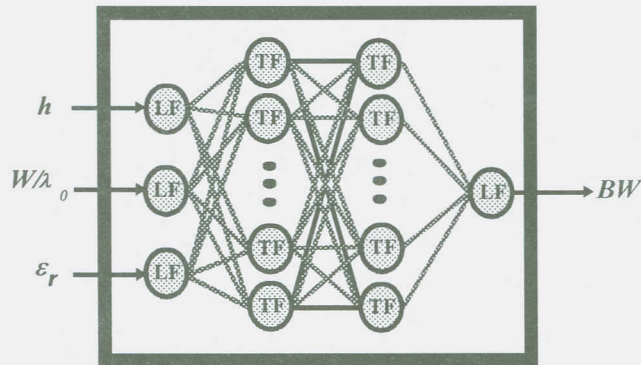


Figure 3. A neural model for bandwidth calculation of a rectangular microstrip antenna

192 train data sets obtained from electric surface current model [6] for $W/\lambda_0=0.1, 0.2, 0.4, 0.5$ and $\epsilon_r = 1.1, 2.2, 9.8$ were used to train the neural models. The unseen 48 data sets for $W/\lambda_0=0.3$ were applied to the network for test. During training, the learning and momentum coefficients were set to 0.01 and 0.1, respectively. The seed number used in the random number generator to initialise the weights of network was fixed to 1.0. The number of training epoch was 20,000. After several trials, the most suitable processing elements numbers for the both hidden layers found were five. Figs. 4-6 and Figs. 7-8 show the training results and the test result, respectively. It can be clearly seen from the figures that the outputs of neural models were almost similar with the data from the Green function methods.

The adaptation in this study has been carried out after the presentation of each set ($h, W/\lambda_0, \epsilon_r$ and BW) until the rms error in learning process was less than 0.009. The rms errors obtained were 0.009 for training and 0.012 for test.

In order to demonstrate the validity of the neural model, the unseen data set to the network obtained from moment method [1,4] for $W/\lambda_0=0.3$ and $\epsilon_r = 2.55$ were also used for test the performance of network. The test results of the model are shown in Fig. 8.

The both test results illustrate that the performances of the networks are quite robust and precise. Thus, the neural models achieve the calculation of the bandwidth for a resonant rectangular microstrip patch antenna with a very good agreement.

In this work, we have not compared the results of neural models with the results of other papers in the literature because all the results reported in the literature agree with those obtained by [4,6]. For this reason, a comparison of the neural model results with the results of other papers is unnecessary.

5. CONCLUSION

A new method based on artificial neural networks trained with the backpropagation algorithm for calculating the bandwidth of both electrically thin and thick rectangular microstrip antennas has been presented. As can be seen from the Figs. 4-8, there is an excellent agreement with the data from the Green function methods. This excellent agreement supports the validity of neural models. When the results of neural models are compared with those by [4,6], the test rms error is within 0.012, which is tolerable for most design applications.

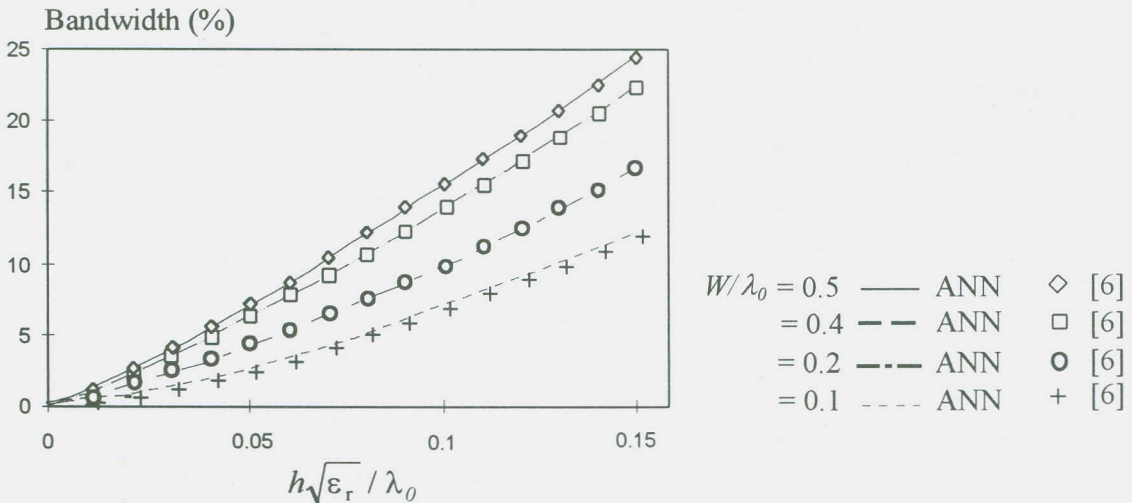


Figure 4. The training results of the bandwidth of a rectangular microstrip antenna as a function of dielectric thickness for $\epsilon_r=1.1$.

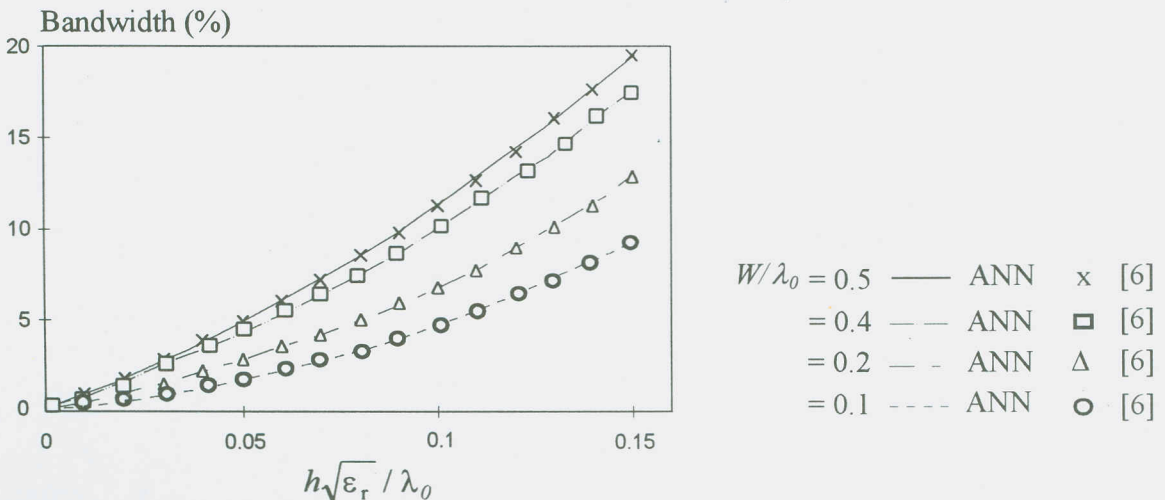


Figure 5. The training results of the bandwidth of a rectangular microstrip antenna as a function of dielectric thickness for $\epsilon_r=2.2$.

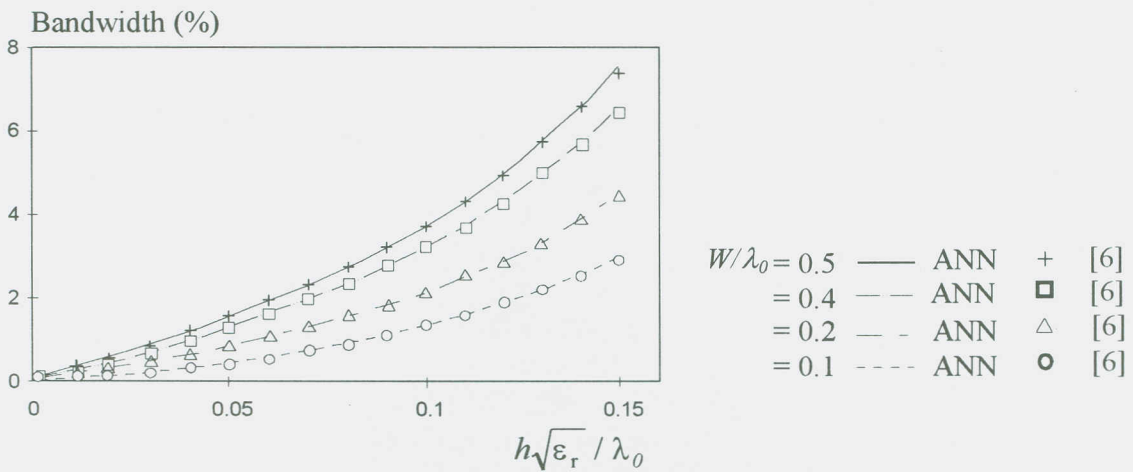


Figure 6. The training results of the bandwidth of a rectangular microstrip antenna as a function of dielectric thickness for $\epsilon_r=9.8$.

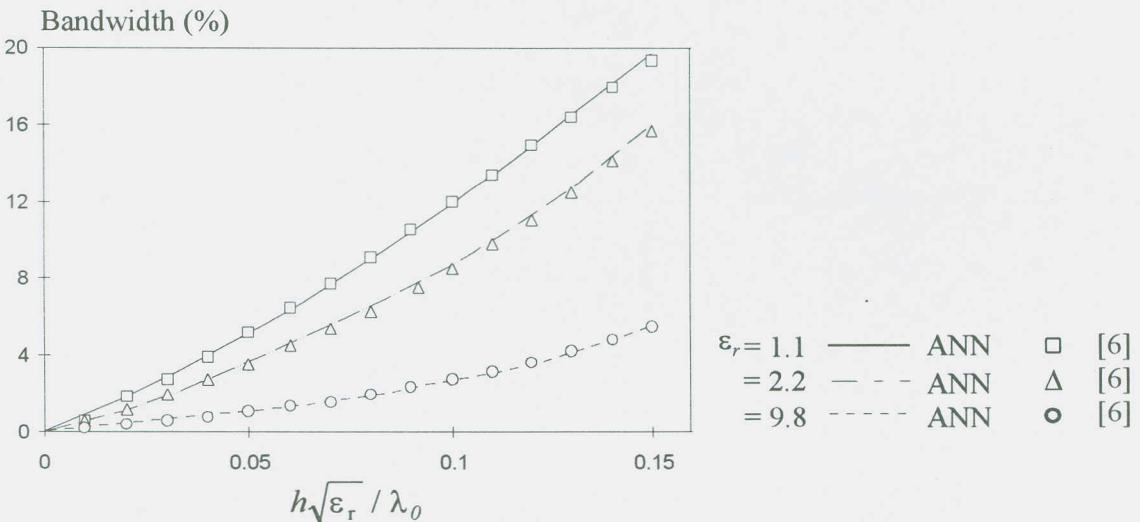


Figure 7. The test results of the bandwidth of a rectangular microstrip antenna as a function of dielectric thickness for $W/\lambda_0=0.3$.

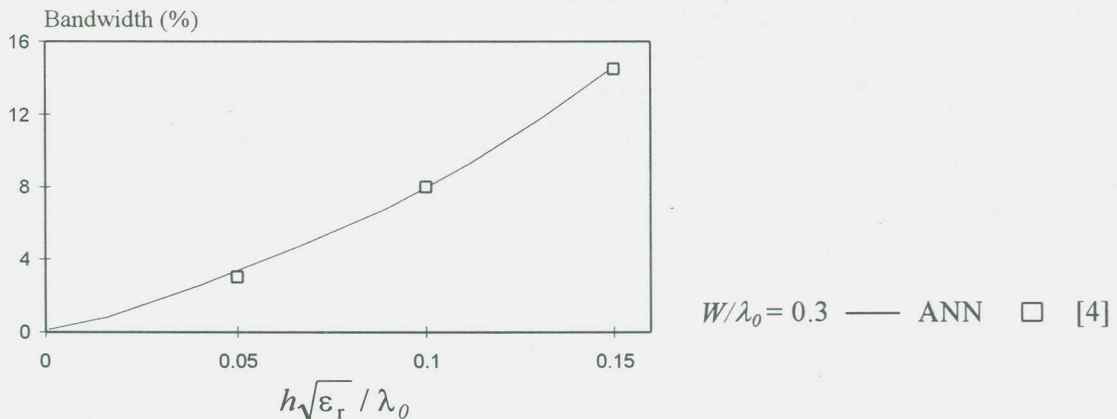


Figure 8. The test results of the bandwidth of a rectangular microstrip antenna as a function of dielectric thickness for $\epsilon_r=2.55$.

Since the neural model presented in this work has high accuracy in the range of $1.1 \leq \epsilon_r \leq 10.0$ and $0 < h/\lambda_0 \leq 0.15$ and requires no complicated mathematical functions, it can be very useful for the development of fast CAD algorithms. This CAD model capable of accurately predicting the bandwidths of rectangular microstrip antennas is also very useful to antenna engineers. Using this model, one can calculate accurately, by a personal computer, the

bandwidth of rectangular patch antennas, without possessing any background knowledge of microstrip antennas. It takes only a few microseconds to produce the bandwidth on a Pentium/100 MHz PC. Even if the training time takes less than ten minutes, after training, the calculation time is less than hundred microseconds in real time calculation. Thus, the neural model is very fast after training.

Finally, we expect that the neural models will find wide applications in CAD of microstrip antennas and microwave integrated circuits.

6. REFERENCES

1. D. M. Pozar and D. H. Schubert (Eds.), *Microwave Antennas: The Analysis and Design of Microstrip Antennas and Arrays*. IEEE Press, New York, 1995.
2. K. R. Carver, Practical analytical techniques for the microstrip antenna, *Proceedings of the Workshop on Printed Circuit Antennas*, New Mexico State University, **29**, 7.1-7.20, 1979.
3. J. Vandensande, H. Pues and A. Van De Capelle, Calculation of the bandwidth of microstrip resonator antennas, *Proceedings of the 9th European Microwave Conference*, 116-119, 1979.
4. D. M. Pozar, Considerations for millimeter wave printed antennas, *IEEE Transactions on Antennas and Propagation*, **31**, 740-747, 1983
5. A. K. Bhattacharyya and R. Garg, Effect of substrate on the efficiency of an arbitrarily shaped microstrip patch antenna, *IEEE Transactions on Antennas and Propagation*, **34**, 1181-1188, 1986.
6. P. Perlmutter, S. Shtrikman and D. Treves, Electric surface current model for the analysis of microstrip antennas with application to rectangular elements, *IEEE Transactions on Antennas and Propagation*, **33**, 301-311, 1985.
7. H. F. Pues and A. Van De Capelle, An impedance-matching technique for increasing the bandwidth of microstrip antennas, *IEEE Transactions on Antennas and Propagation*, **37**, 1345-1354, 1989.
8. K. Güney, 1994c, Bandwidth of a resonant rectangular microstrip antenna, *Microwave and Optical Technology Letters*, **7**, 521-524;
9. K. Güney, Comments on 'On the resonant frequencies of microstrip antennas', *IEEE Transactions on Antennas and Propagation*, **42**, 1363-1365; 1994.
10. K. Güney, Resonant frequency of a tunable rectangular microstrip patch antenna, *Microwave and Optical Technology Letters*, **7**, 581-585; 1994.
11. K. Güney, Space wave efficiency of electrically thick circular microstrip antennas, *International Journal of Electronics*, **78**, 571-579; 1995.
12. K. Güney, Closed-form expression for radiation resistance of a resonant rectangular microstrip patch antenna, *International Journal of Microwave and Millimeter-Wave Computer-Aided Engineering*, **5**, 31-39, 1995.
13. A. Maren, C. Harston and R. Pap, *Handbook of Neural Computing Applications*, Academic Press, London, ISBN 0-12-471260-6, 1990.
14. S. Haykin, *Neural Networks: A Comprehensive Foundation*, ISBN 0-02-352761-7, Macmillan College Publishing Company, New York, USA, 1994.
15. S. Sagiroglu and K. Güney, Calculation of resonant frequency for an equilateral triangular microstrip antenna using artificial neural networks. *Microwave and Optical Technology Letters*, **14**, 89-93, 1997.
16. S. Sagiroglu, K. Güney, and M. Erler, Neural network calculation of radiation resistance of a rectangular microstrip antenna, *TAINN'97*, 211-215, 1997.
17. S. Sagiroglu, K. Güney, and M. Erler, Resonant frequency calculation for circular microstrip antennas using artificial neural networks, *International Journal of Microwave and Millimeter-Wave Computer-Aided Engineering*, Special issue, **8(3)**, 220-227, 1998.

18. S. Sagiroglu, K. Güney, and M. Erler, Neural network calculation of radiation resistance of a rectangular microstrip antenna, *TAINN'98*, 1998.
19. D. E. Rumelhart and J. L. McClelland, *Parallel Distributed Processing*, Vol. 1, The MIT Press, Cambridge, 1986.
20. R. P. Gorman and T. J. Sejnowski, Analysis of hidden units in a layered network trained to classify sonar targets, *IEEE Transactions on Neural Networks*, **1**, 75-89, 1988.
21. Y. V. Cherkassky and N. Vassilas, Back-propagation networks for spelling correction, *IEEE Transactions on Neural Networks*, **1**, 166-173, 1989.
22. S. Sagiroglu, Modelling a robot sensor using artificial neural networks, *PhD Thesis, University of Wales, Systems Engineering Department, Cardiff*, 1994.
23. G. Chandani and W. Cao, On hidden nodes for neural nets. *IEEE Transactions on Circuits and Systems*, **36**, 661-664, 1989.
24. D. L. Chester, Why two hidden layers are better than one, *Proceedings of International Joint Conference on Neural Networks*, Washington, DC., **1**, 265-268, 1990.
25. W. Y. Huang and Y. F. Huang, Bounds on the number of hidden neurons in multilayered perceptron, *IEEE Transactions on Neural Networks*, **1**, 47-55, 1991.